

***Hibiscus sabdariffa* Inhibits Vascular Smooth Muscle Cell Proliferation and Migration Induced by High Glucose—A Mechanism Involves Connective Tissue Growth Factor Signals**

CHIEN-NING HUANG,[†] KUEI-CHUAN CHAN,[†] WEI-TING LIN,[‡] SHI-LI SU,[§]
 CHAU-JONG WANG,^{*,‡,⊥} AND CHIUNG-HUEI PENG^{*,||,⊥}

Department of Internal Medicine, Chung-Shan Medical University Hospital, School of Medicine, and Institute of Biochemistry and Biotechnology, Chung-Shan Medical University, Number 110, Section 1, Chien-Kuo North Road, Taichung 402, Taiwan, Division of Endocrinology and Metabolism, Department of Internal Medicine, Changhua Christian Hospital, 135 Nanxiao Street, Changhua City, Changhua County 500, Taiwan, and Division of Basic Medical Science, Hungkuang University, Number 34, Chung Chie Road, Shalu County, Taichung County 433, Taiwan

Recently, the herbal extract of *Hibiscus sabdariffa* was shown to have multiple bioactive effects, including anti-atherosclerosis. On the basis of this, we aimed to examine whether the polyphenolic isolate of *H. sabdariffa* (HPI) could protect high-glucose-treated vascular smooth muscle cell (VSMC) and its putative transduction signals. Results showed that HPI dose- and time-dependently reduced the high-glucose-stimulated cell proliferation and migration. HPI suppressed the proliferating cell nuclear antigen (PCNA) level and matrix metalloproteinase (MMP)-2 activation. In addition, the expressions of connective tissue growth factor (CTGF) and receptor of advanced glycation end product (RAGE) enhanced by high glucose were prominently suppressed by HPI. The proliferation signal mediated by high glucose was demonstrated via CTGF/RAGE, while MMP-2 was regulated by CTGF but not RAGE. Conclusively, the results suggest that HPI potentially can be a promising adjuvant herbal therapy for diabetic patients.

KEYWORDS: *Hibiscus sabdariffa* polyphenolic isolate; high glucose; vascular smooth muscle cell; connective tissue growth factor; receptor of advanced glycation end product

INTRODUCTION

Diabetes mellitus is a worldwide, high prevalent disease with a consistent increase of mortality, mainly because of coronary heart disease (1). The coronary vascular lesion is characterized as atheroma resulted from endothelial damage, oxidized low-density lipoprotein (LDL) infiltration, macrophage activation, collagen deposition, and the proliferation and migration of vascular smooth muscle cells (VSMCs) (2).

A high-glucose condition had been shown to mediate the growth and extracellular matrix (ECM) gene expression of VSMC (3), to promote the anti-apoptotic signaling of VSMC during neointima lesion formation (4), and to potentiate VSMC

chemotaxis and migration (5). In addition, it also enhanced the responses to PDGF and TGF- β through a tyrosine kinase receptor (6). Hyperglycemia promotes the formation of advanced glycation end product (AGE) (7). Interacting with its specific receptor (RAGE), AGE is suggested to play a role in atherosclerotic plaque formation, which could be reduced by the AGE inhibitor in the diabetic rat model (8).

The cysteine-rich secreted peptide connective tissue growth factor (CTGF) was reported to be involved in fibroblast proliferation, migration, attachment, and ECM formation and remodeling. CTGF showed that it exerts its regulation in various cell lines including VSMC by stimulating its proliferation and migration (9), suggesting that it is involved in atherosclerosis and diabetic nephropathy (10, 11).

Hibiscus sabdariffa L. (HS), a native tropical plant, is widely cultivated in Eastern Taiwan and commonly used as local soft drink. Traditionally, it has been used effectively against hypertension, inflammation, and liver disorders (12). Previous studies of our research team showed that *H. sabdariffa* possessed multi-effects acting on anti-tumor, anti-oxidation, and anti-hyperlipidemia. Recently, it was reported that the extract of *H. sabdariffa* inhibited the LDL oxidation and lowered serum

* To whom correspondence should be addressed. Telephone: +866-4-26318652 ext. 7065. Fax: +866-4-24715926. E-mail: kenny.huangcn@msa.hinet.net (C.-H.P.).

[†] School of Medicine, Chung-Shan Medical University.

[‡] Institute of Biochemistry and Biotechnology, Chung-Shan Medical University.

[§] Changhua Christian Hospital.

^{||} Hungkuang University.

[⊥] These authors contributed equally to this work and therefore share corresponding authorship.

triacylglyceride, cholesterol, and LDL-cholesterol in animal experiments (13–15). Histological examination revealed that it could reduce foam cell formation and inhibit VSMC proliferation and migration, suggesting the anti-atherosclerotic effect of *H. sabdariffa*.

In the present study, an *in vitro* model was used to deduce if glucose could induce VSMC proliferation and migration and the possible signals involved. Furthermore, whether the polyphenolic isolate of *H. sabdariffa* (HPI) could exert the protective effect on VSMC will also be investigated.

MATERIALS AND METHODS

Chemicals. Minimal essential media, fetal calf serum, penicillin, and streptomycin were purchased from Gibco BRL (Grand Island, NY). Sodium dodecyl sulfate (SDS), bis-acrylamide, ammonium persulfate, *N,N,N',N'*-tetramethylethylenediamine (TEMED), and nitrocellulose membrane came from Bio-Rad Laboratories (Hercules, CA). Tris-HCl, anti-actin, and anti-mouse IgG came from Sigma Chemical Co. (St. Louis, MO). Antibodies of CTGF, RAGE, and proliferating cell nuclear antigen (PCNA) were from Santa Cruz Biotechnology (Santa Cruz, CA). Small interfering RNA (siRNA) for CTGF was synthesized by Thermo Fisher Scientific, Inc.; ON-TARGETplus SMARTpool siRNA L-080139-01-0010, rat CTGF, NM_022266; target sequence: GUAUGGAGACAUUGGCGUAA, UAUGGUACGUAGACGGUAA, AGACACUGGUUCGAGACA, and GGAGUAAGGGACACGAACU.

Source of Polyphenolic Isolate of *H. sabdariffa* L. The HPI was gifted by Dr. Lin of our laboratory (13).

High-Performance Liquid Chromatography (HPLC) Assay for HPI. The components of HPI were determined by HPLC (Hitachi L-4250 UV-vis detector; L-6200A Intelligent Pump) analysis using 5 μ m symmetry shield RP18 reverse-phase column (Kanto Chemical Co., Inc.; *l* = 250 mm, inner diameter = 2.5 mm) and an UV detector monitored at 260 nm. The samples were filtered through a 0.45 μ m filter disk, and 20 μ L of HPI (10 mg/mL) was injected into the column. The mobile phase contained two solvents (A, acetic acid/water = 20:980; B, acetic acid/water/acetonitrile = 2.5:497.5:500). At room temperature, the process ran by a linear gradient method from 20 to 85% B (flow rate = 1 mL/min) over 70 min.

Cell Culture. The rat aortic smooth muscle cells (A7r5 cells) were maintained in Dulbecco's modified Eagle's medium supplemented with 10% fetal calf serum and 1% penicillin at 37 °C in a humidified atmosphere with 5% CO₂. Cells were seeded at a density of 5×10^5 cells onto each 10 mm Petri dish 24 h before drug treatment.

Migration Assay. The *in vitro* migratory activity of VSMCs was measured using a wound migration assay. Cells were seeded at 5×10^5 cells/well in a 6-well plate and obtained 50–70% confluence. An injury line was created with a single scratch at the center of a VSMC monolayer (50–70% confluence) using a sterile 1.15 mm diameter pipet tip. Thereafter, VSMCs were continuously cultured and photographed with phase-contrast microscopy (model CK40, Olympus) at 24, 48, and 72 h, respectively, with five images of randomly selected field for each preparation. The distance between cells at both sides of the wound was measured for five pairs of cells per image. Cell migration was expressed in the percentage of initial wound width.

siRNA Transfection. A7r5 cells were seeded at 2×10^5 cells/well in 6-well plates and incubated for 24 h. A total of 500 μ L of serum and PS-free medium containing 0, 0.5, and 1 nmol of mismatched siRNA (siRNA for CTGF of rats), respectively, were mixed with 500 μ L of serum and PS-free medium containing 10 μ L of Lipofectamine2000 as the cationic liposomal gene transfection reagent. The mixture was then added with 9 mL of serum and PS-free medium, standing for 1 h. Cells were washed with PBS, then added with 2 mL of mixture/well, and incubated for 12 h. The mixture was subsequently replaced with normal cultured medium and incubated for another 12 h. After that, cells were treated with different conditions. The cell proteins were then extracted and prepared for immunoblotting.

Electrophoresis and Immunoblotting. Cells were harvested into lysis buffer containing 50 mM Tris-HCl (pH 6.8), 10% glycerol, 2% SDS, and 5% mercaptoethanol and then lysed by sonication. Equal

amounts of protein (50 mg/lane) were subjected to SDS-polyacrylamide gel electrophoresis (SDS-PAGE) and then transfected to nitrocellulose (NC) membranes. Subsequently, NC membranes were blocked with 5% bovine serum albumin with 0.05% Tween 20 in phosphate-buffered saline and then were incubated with the first antibody for 1 h. NC membranes were washed 3 times with 0.05% Tween 20 in phosphate-buffered saline and incubated with the secondary antibody conjugated to anti-mouse horseradish peroxidase (Amersham Life Science, Buckinghamshire, U.K.). Bands were visualized using the enhanced chemiluminescent (ECL) Western blotting detection system (Perkin-Elmer Life Sciences, Boston, MA). Protein quantities were determined by densitometry through AlphaImager Series 2200 software (Alpha Innotech, San Leandro, CA).

Zymography. The cultured media were collected for analyzing the protein masses bearing gelatin activity by zymography. A SDS-PAGE containing 0.1% gelatin was prepared. Medium samples were resolved on the gel, which was then washed twice with 2.5% Triton-X 100 solution for 30 min, with gentle shaking to remove SDS. The washed gel was placed in the development buffer solution, consisting of 150 mM NaCl in 20 mM Tris-HCl at pH 7.4, and incubated for 16 h at 37 °C. After the incubation, the gel was washed and stained with Coomassie Brilliant Blue R-250. The protein bands bearing gelatin proteolytic activity appeared as translucent in a blue-stained background.

Statistics. Data were presented as means \pm standard deviation (SD). Statistical differences were evaluated using the unpaired *t* test and considered significant at the *p* < 0.05 level.

RESULTS

Composition of HPI. Figure 1 showed the HPLC chromatogram of HPI. The presence and proportion of the main constituents of HPI were protocatechuic acid (24.24%), catechin (2.67%), epigallocatechin (2.44%), caffeic acid (19.85%), and epigallocatechin gallate (27.98%).

Effect of HPI on the Proliferation of VSMC Induced by High Glucose. In Figure 2, after treatment for 48 h, A7r5 cell growth was significantly stimulated by a high-glucose (25 mM) condition when compared to the control. High glucose increased the cell growth about 2- and 2.5-folds at 72 and 96 h, respectively, which was inhibited dose-dependently by HPI. Among all of the concentrations, 1 mg/mL HPI revealed a complete inhibition.

Effect of HPI on the Migration of VSMC Induced by High Glucose. Figure 3 showed that high glucose induced the cell migration above 2-fold, whereas HPI dose-dependently inhibited its migration. At a concentration of 1 mg/mL, HPI even significantly reduced about 80% of migration induced by high glucose. In addition, high glucose increased cell migration time-dependently. The migration was found to be enhanced almost 3-folds until 72 h, whereas it was time-dependently inhibited by HPI.

Effect of HPI on the Expression of PCNA, CTGF, and RAGE Induced by High Glucose. To further investigate if high glucose could induce A7r5 cell proliferation and what could be the target affected by HPI, cells were treated with high glucose with or without HPI. Figure 4 showed that PCNA, the marker of proliferation, was increased about 80% at 72 h, the time break at which significant growth deviation was observed (Figure 2). HPI had inhibited the expression of PCNA and the high-glucose-induced cell proliferation dose-dependently, implicating the regulatory effect of HPI on PCNA.

To investigate whether AGE was involved in high-glucose-induced cellular changes and regulated by HPI, we observed the expression of AGE-specific receptor, RAGE. In addition, because of the involvement of CTGF in atherosclerosis and

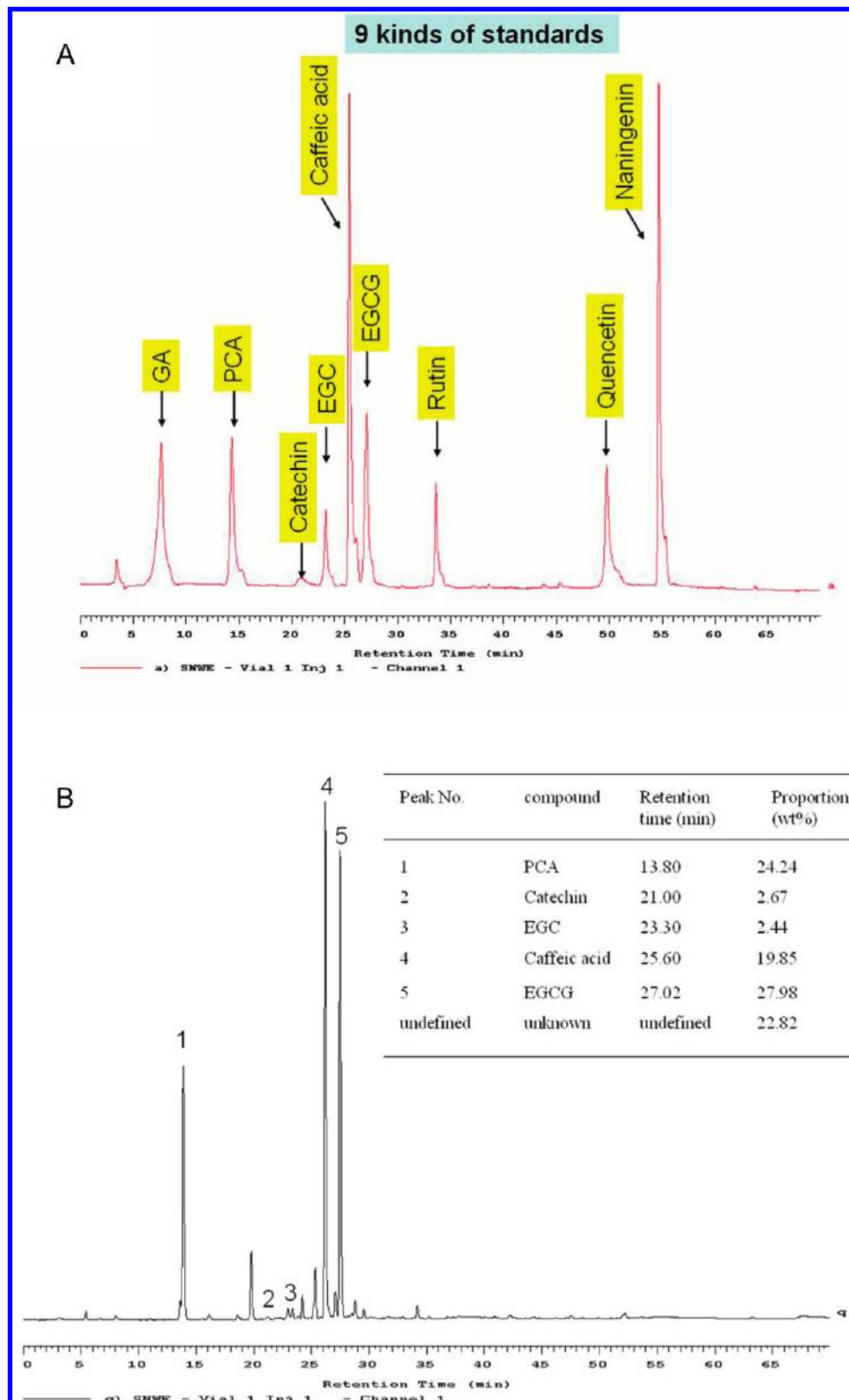


Figure 1. HPLC analysis of HPI. (A) Standards comprised nine kinds of standard polyphenols (1 mg/mL): gallic acid (GA), protocatechuic acid (PCA), catechin, epigallocatechin (EGC), caffeic acid, epigallocatechin gallate (EGCG), rutin, quercetin, and naringenin. The retention time of each component was determined by HPLC analysis under the same condition as described. (B) HPLC chromatogram of free polyphenols from HPI (10 mg/mL). When the retention time was compared, these phenolic components correspond to five peaks shown in A. The percentage of composition is shown in the inset.

the proliferation and migration of VSMC, we also observed CTGF expression in cells treated with different conditions. **Figure 4** showed that both levels of RAGE and CTGF were increased approximately 2-fold by high-glucose treatment. Meanwhile, HPI decreased the levels of RAGE and CTGF

in a dose-dependent manner, implying that RAGE and CTGF might be closely involved in the signal transduction pathway transduced by high glucose and HPI.

CTGF Was Involved in High-Glucose-Stimulated Expression of PCNA and RAGE. High-glucose-induced PCNA

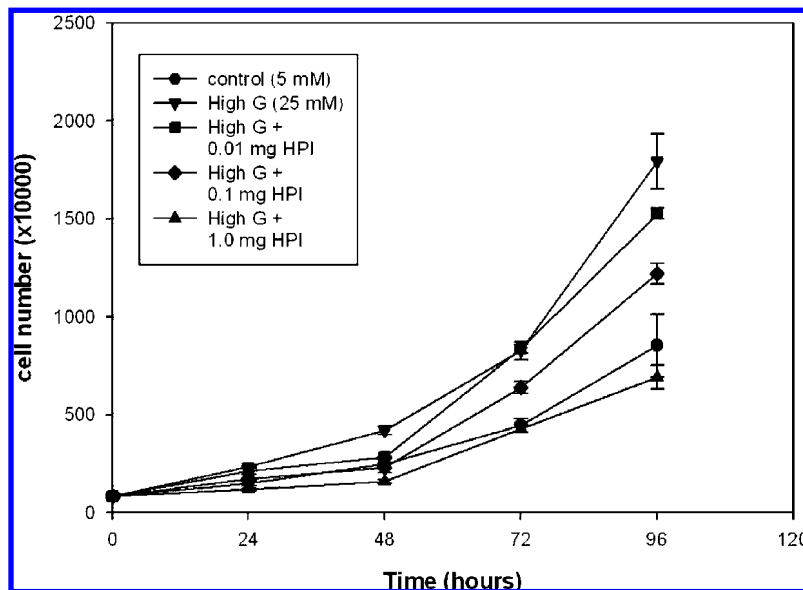


Figure 2. HPI suppresses the high-glucose-induced growth. A7r5 cells were treated with 25 mM glucose with or without various concentrations of HPI at the indicated time. The values are means \pm SD, $n = 3$.

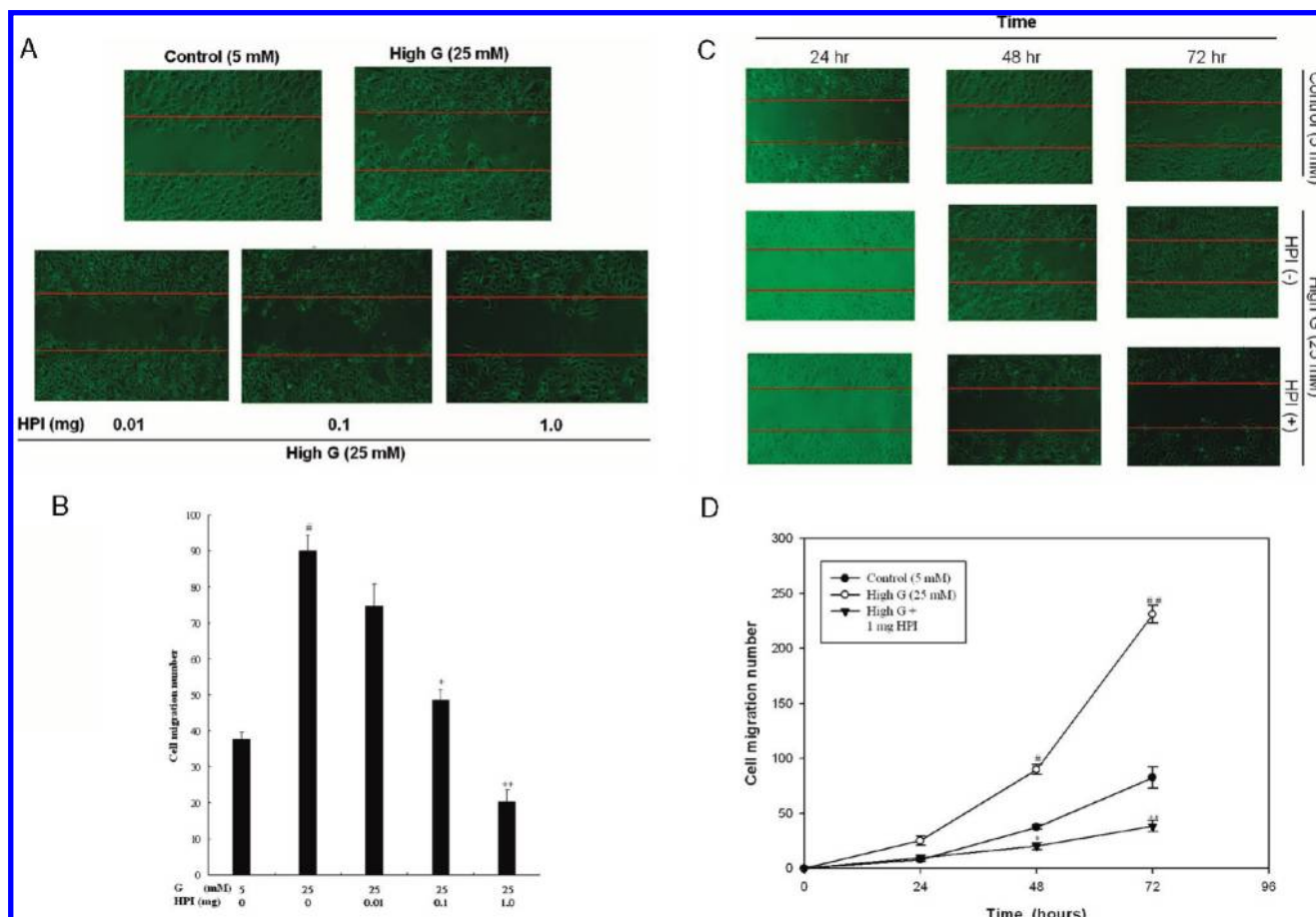


Figure 3. HPI suppresses the high-glucose-induced migration. (A) A7r5 cells were treated with 25 mM glucose with various concentrations of HPI at 48 h (photograph magnification, 400 \times). (B) Bar graph showed the results of A. Data were presented as means \pm SD, $n = 3$, (#) $p < 0.001$, compared to the control group; (*) $p < 0.005$ and (**) $p < 0.001$, compared to the high-glucose-treated group. (C) Cells were treated with 25 mM glucose with or without 1 mg of HPI at the indicated time (photograph magnification, 400 \times). (D) Growth curve showed the results of C. The values are means \pm SD, $n = 3$. (#) $p < 0.005$ and (##) $p < 0.001$, compared to the control group; (*) $p < 0.005$ and (**) $p < 0.001$, compared to the high-glucose-treated group.

expression was apparently inhibited by CTGF siRNA (Figure 5), suggesting that CTGF could be involved in the mediation

of high-glucose-induced cell proliferation. In addition, CTGF was also involved in RAGE expression (Figure 5). Because

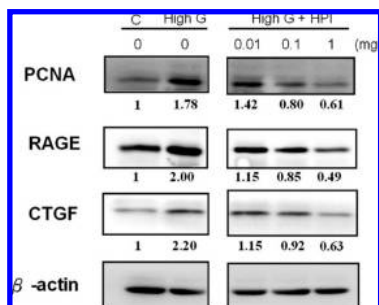


Figure 4. HPI suppresses the high-glucose-induced PCNA, CTGF, and RAGE. Cells were treated with 25 mM glucose with or without various concentrations of HPI at 72 h. The expressions of PCNA, CTGF, and RAGE were analyzed by a Western blot and densitometer. Three independent experiments were conducted, all showing similar patterns of changes.

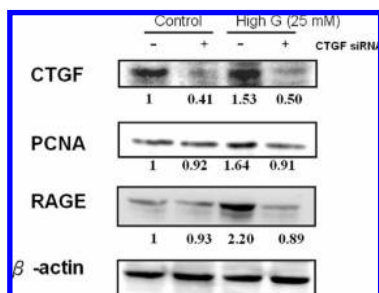


Figure 5. CTGF mediates the high-glucose-induced elevation of PCNA and RAGE. Cells were treated with 25 mM glucose at 72 h with or without CTGF siRNA. The expressions of PCNA and RAGE were analyzed by a Western blot and densitometer. Three independent experiments were conducted, all showing similar patterns of changes.

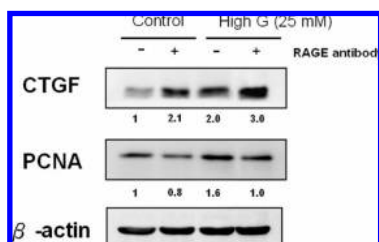


Figure 6. RAGE mediates the high-glucose-induced elevation of PCNA. Cells were treated with 25 mM glucose at 72 h with or without RAGE antibody. The expressions of PCNA and CTGF were analyzed by a Western blot and densitometer. Three independent experiments were conducted, all showing similar patterns of changes.

HPI had simultaneously inhibited the expressions of both CTGF and RAGE (**Figure 4**), an implication revealed that HPI could exert its protective effect through modulation of both CTGF and RAGE, resulting in suppressed cell proliferation.

RAGE Mediated Downstream of CTGF in High-Glucose-Stimulated Cell Proliferation. RAGE antibody was used to test if PCNA could be influenced by RAGE inhibition. It was found that high-glucose-induced PCNA elevation was abolished by RAGE antibody. However, the expression of CTGF was not regulated by RAGE blockage (**Figure 6**). In comparison, the results shown in **Figures 5** and **6** indicated that RAGE mediated the downstream of CTGF in high-glucose-induced proliferation. Hence, HPI could exert its anti-proliferation effect through regulation of CTGF/RAGE.

Effect of HPI on the Expression of MMP-2 Induced by High Glucose. Matrix metalloproteinase (MMP) is the ECM-degrading enzyme during the process of migration, which could

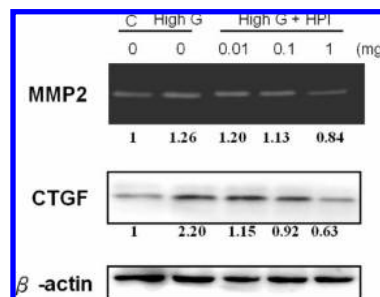


Figure 7. HPI suppresses the high-glucose-activated MMP-2. Cells were treated with 25 mM glucose with or without various concentrations of HPI at 24 h. The expressions of MMP-2 contained in culture medium were analyzed by zymography. Three independent experiments were conducted, all showing similar patterns of changes (The expression of CTGF is the same shown in **Figure 4**).

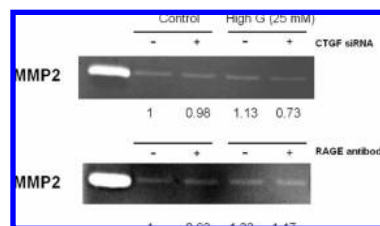


Figure 8. CTGF mediates the high-glucose-induced MMP-2 activation. Cells were treated with 25 mM glucose with or without CTGF siRNA or RAGE antibody, respectively. After treatment, the expressions of MMP-2 secreted into culture medium were analyzed by zymography. Three independent experiments were conducted, all showing similar patterns of changes.

be secreted to the cultured medium. Our data demonstrated that high glucose induced the activation of MMP-2 (**Figure 7**), which was further inhibited by HPI. In addition, the expressions of CTGF were found to be parallel to those of MMP-2, implying that CTGF might be involved in the cell migration.

CTGF Was Involved in High-Glucose-Stimulated Activation of MMP-2. CTGF siRNA or RAGE antibody was used, respectively, to detect if MMP-2 could be influenced. **Figure 8** showed that high-glucose-induced MMP-2 activation was inhibited by CTGF siRNA, suggesting that CTGF mediated high-glucose-induced cell migration. However, MMP-2 was not regulated by RAGE blockage, indicating that RAGE was not involved in cell migration. In summary, this evidence showed that HPI could exert its protective effect through downstream regulation of CTGF and, subsequently, influenced the migration.

DISCUSSION

In the present study, using the *in vitro* cell culture model, the results demonstrate that high glucose per se induces the expression of CTGF and, subsequently, mediates the proliferation and migration of VSMC, while HPI downregulates CTGF and inhibits the high-glucose-induced cellular changes (**Figure 9**).

It had been shown that high-glucose-induced upregulation of CTGF mRNA appeared to be TGF- β -dependent, because TGF- β antibody blocked the expression of CTGF and the downstream ECM protein accumulation in VSMC (16). High glucose triggered the CTGF expression via TGF- β_1 and protein kinase C in mesangial cells and thus mediated the matrix production, indicating that CTGF played an important role in diabetic nephropathy (17).

Our data suggest that CTGF mediates high-glucose-induced cell proliferation via AGE/RAGE. This result is different from

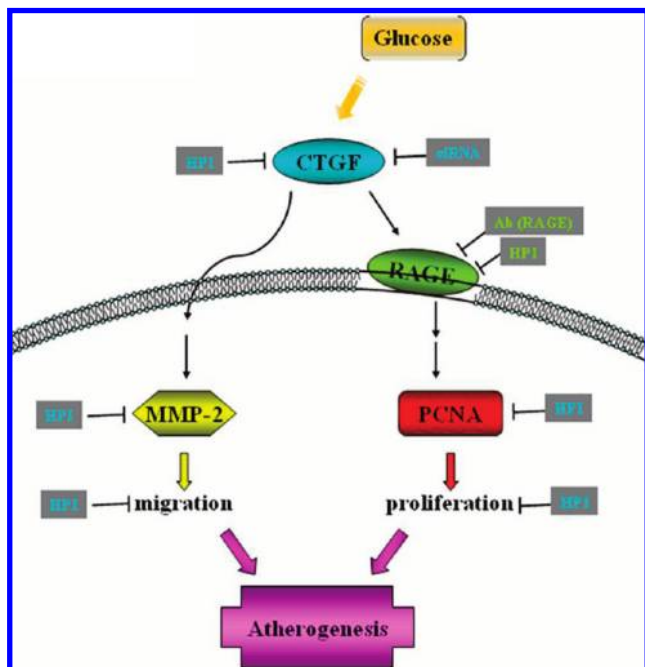


Figure 9. HPI inhibits the high-glucose-induced cellular changes via regulation of CTGF.

the other investigations. In the literature, AGE-induced tubular epithelial–mesenchymal transition via CTGF (18). AGE induced mitogenesis and collagen production of NRK-49F cells through the regulation of angiotensin II and CTGF (19). In contrast, our data show that CTGF regulates the downstream AGE receptor and then increases the expression of PCNA.

It has been demonstrated that AGE/RAGE was a critical mediator in diabetic skin. AGE/RAGE was associated with the decrease of PCNA. Application of RAGE-blocking antibody redressed high-glucose-induced cell cycle arrest and apoptosis (20). RAGE was involved in the diabetic-associated impairment of angiogenesis. In insulin-deficient wild-type mice, PCNA-positive cells were significantly diminished, whereas this alteration was not found in RAGE (−/−) mice (21), providing evidence of the intimate correlation between RAGE and the regulation of PCNA. However, in comparison to our data, the decrease of PCNA in other studies could result from the variation in cell types, tissues, and experiment designs.

Our results also show that CTGF activated MMP-2 and promoted the migration of VSMC, whereas RAGE was not involved in MMP-2 activation. According to the report of Yang et al., CTGF suppressed TIMP-2 and increased MMP-2 through ERK1/2 activation (22). In the high-glucose-induced human brain cells, CTGF increased MMP-2 mRNA, although it also increased TIMP-1 to inhibit ECM degradation (23).

Many previous reports had indicated that MMP-2 plays an important role in atherosclerosis and the migration of VSMC. Using an immunohistochemical stain to analyze the atherosclerotic lesion of high-cholesterol food-fed rabbits, Kuge et al. observed that MMP-2, MT-1, and Cox-2 co-distributed on the macrophage-riched instable plaque (24). In hemodialyzed patients complicated with vascular diseases, the increased serum MMP-2 and Cu/Zn SOD was associated with intima mediate thickness (25). Besides, the extrinsic coagulation pathway and MMP-2/TIMPs system could exert a synergistic effect to form atherosclerosis while stimulated with oxidative stress. It reveals that MMP-2 promotes the vascular aging via TGF- β and TGF- β ₁-type II receptor (26). Furthermore, because leptin increases in diabetes, it might be associated with vascular complications.

In the previous report, leptin was demonstrated to induce the signals of PKC/NADPH/ERK/NF- κ B and thus promoted the proliferation and MMP-2 expression of aortic smooth muscle cells (27). However, in the high-glucose conditions, the mechanism mediating MMP activation and the downstream signals regulated by MMP have yet to be clarified. It had been shown that high glucose potentiated VSMC chemotaxis via activation of PI3K and MAPK (5). PTEN were also reported to be involved in VSMC migration (28). Further investigation is needed to illustrate the transduction pathways of high-glucose-induced MMP.

In humans, high glucose induces reactive oxygen species (ROS) generation via the oxygen-consuming process in mitochondria, thereby stimulating the activation of NF- κ B and production of IL-1 and TNF- α (29). These inflammatory cytokines are involved in a variety of cell responses, for example, injury of β -islets or impeding the insulin receptor and related signal transduction. Because oxidative stress and inflammatory cells are involved in the pathogenesis of atherosclerosis, high glucose would be expected to promote vascular changes through inflammatory cytokines and the transduced signals. It had been revealed that high glucose stimulated TNF- α -induced expression of NF- κ B via GSH reduction and PKC activation (30). High glucose enhanced IL-1-induced Cox-2 activation and resulted in the production of prostaglandin (31).

In the present study, HPI demonstrates its protective effect under high-glucose conditions. It has been shown that the *H. sabdariffa* extract inhibited LDL oxidation and reduced foam cell formation and migration of VSMC (15). In the clinical test, the extract had been shown to reduce serum cholesterol (14). *Hibiscus* anthocyanin-rich extract induced apoptotic cell death in human leukemia cells and VSMC via activation of p38 MAPK and p53 (32). HPI induced apoptosis in human gastric carcinoma cells via p53 phosphorylation and p38 MAPK/Fas L cascade pathway (13). HPLC analysis showed that at least five polyphenols were contained in HPI.

Recently, the ethanolic extract of *H. sabdariffa* showed its hypolipidemic and antioxidant effects in alloxan-induced diabetic rats. To summarize, *H. sabdariffa* is worthy of being further investigated and could potentially be developed as an adjunctive therapeutic for diabetes or metabolic syndrome.

ABBREVIATIONS USED

HPI, *H. sabdariffa* polyphenolic isolate; VSMC, vascular smooth muscle cell; CTGF, connective tissue growth factor; RAGE, receptor of advanced glycation end product; PCNA, proliferating cell nuclear antigen; MMP, matrix metalloproteinase; siRNA, small interfering RNA.

ACKNOWLEDGMENT

The authors acknowledge Dr. Hui-Hsuan Lin for providing the HPI.

LITERATURE CITED

- (1) Mueck, A. O.; Seeger, H. Estrogens acting as cardiovascular agents: Direct vascular actions. *Curr. Med. Chem. Cardiovasc. Hematol. Agents* **2004**, *2*, 35–42.
- (2) Glass, C. K.; Witztum, J. L. Atherosclerosis. The road ahead. *Cell* **2001**, *104*, 503–516.
- (3) Sharpe, P. C.; Yue, K. K.; Catherwood, M. A.; McMaster, D.; Trimble, E. R. The effects of glucose-induced oxidative stress on growth and extracellular matrix gene expression of vascular smooth muscle cells. *Diabetologia* **1998**, *41*, 1210–1219.

- (4) Hall, J. L.; Chatham, J. C.; Eldar-Finkelman, H.; Gibbons, G. H. Upregulation of glucose metabolism during intimal lesion formation is coupled to the inhibition of vascular smooth muscle cell apoptosis. Role of GSK3 β . *Diabetes* **2001**, *50*, 1171–1179.
- (5) Campbell, M.; Allen, W. E.; Silversides, J. A.; Trimble, E. R. Glucose-induced phosphatidylinositol 3-kinase and mitogen-activated protein kinase-dependent upregulation of the platelet-derived growth factor- β receptor potentiates vascular smooth muscle cell chemotaxis. *Diabetes* **2003**, *52*, 519–526.
- (6) Little, P. J.; Allen, T. J.; Hashimura, K.; Nigro, J.; Farrelly, C. A.; Dilley, R. J. High glucose potentiates mitogenic responses of cultured ovine coronary smooth muscle cells to platelet derived growth factor and transforming growth factor- β 1. *Diabetes Res. Clin. Pract.* **2003**, *59*, 93–101.
- (7) Wautier, J. L.; Guillausseau, P. J. Advanced glycation end products, their receptors and diabetic angiopathy. *Diabetes Metab.* **2003**, *27*, 535–542.
- (8) Forbes, J. M.; Yee, L. T.; Thallas, V.; Lassila, M.; Candido, R.; Jandeleit-Dahm, K. A.; Thomas, M. C.; Burns, W. C.; Deemer, E. K.; Thorpe, S. R.; Cooper, M. E.; Allen, T. J. Advanced glycation end product interventions reduce diabetes-accelerated atherosclerosis. *Diabetes* **2003**, *53*, 1813–1823.
- (9) Shi-Wen, X.; Leask, A.; Abraham, D. Regulation and function of connective tissue growth factor/CCN2 in tissue repair, scarring and fibrosis. *Cytokine Growth Factor Rev.* **2008**, *19*, 133–144.
- (10) Jedsadayanmata, A.; Chen, C. C.; Kireeva, M. L.; Lau, L. F.; Lam, S. C. Activation-dependent adhesion of human platelets to Cyr61 and Fisp12/mouse connective tissue growth factor is mediated through integrin $\alpha_{IIb}\beta_3$. *J. Biol. Chem.* **1999**, *274*, 24321–24327.
- (11) Riser, B. L.; Denichilo, M.; Cortes, P.; Baker, C.; Grondin, J. M.; Yee, J.; Narins, R. G. Regulation of connective tissue growth factor activity in cultured rat mesangial cells and its expression in experimental diabetic glomerulosclerosis. *J. Am. Soc. Nephrol.* **2000**, *11*, 25–38.
- (12) Wang, C. J.; Wang, J. M.; Lin, W. L.; Chu, C. Y.; Chou, F. P.; Tseng, T. H. Protective effect of *Hibiscus* anthocyanins against tert-butyl hydroperoxide-induced hepatic toxicity in rats. *Food Chem. Toxicol.* **2000**, *38*, 411–416.
- (13) Lin, H. H.; Huang, H. P.; Huang, C. C.; Chen, J. H.; Wang, C. J. *Hibiscus* polyphenol-rich extract induces apoptosis in human gastric carcinoma cells via p53 phosphorylation and p38 MAPK/FasL cascade pathway. *Mol. Carcinog.* **2007**, *43*, 86–99.
- (14) Lin, T. L.; Lin, H. H.; Chen, C. C.; Lin, M. C.; Chou, M. C.; Wang, C. J. *Hibiscus sabdariffa* extract reduces serum cholesterol in men and women. *Nutr. Res.* **2007**, *27*, 140–145.
- (15) Chen, C. C.; Hsu, J. D.; Wang, S. F.; Chiang, H. C.; Yang, M. Y.; Kao, E. S.; Ho, Y. C.; Wang, C. J. *Hibiscus sabdariffa* extract inhibits the development of atherosclerosis in cholesterol-fed rabbits. *J. Agric. Food Chem.* **2003**, *51*, 5472–5477.
- (16) Liu, X.; Luo, F.; Pan, K.; Wu, W.; Chen, H. High glucose upregulates connective tissue growth factor expression in human vascular smooth muscle cells. *BMC Cell Biol.* **2007**, *8*, 1.
- (17) Murphy, M.; Godson, C.; Cannon, S.; Kato, S.; Mackenzie, H. S.; Martin, F.; Brady, H. R. Suppression subtractive hybridization identifies high glucose levels as a stimulus for expression of connective tissue growth factor and other genes in human mesangial cells. *J. Biol. Chem.* **1999**, *274*, 5830–5834.
- (18) Burns, W. C.; Twigg, S. M.; Forbes, J. M.; Pete, J.; Tikellis, C.; Thallas-Bonke, V.; Thomas, M. C.; Cooper, M. E.; Kantharidis, P. Connective tissue growth factor plays an important role in advanced glycation end product-induced tubular epithelial-to-mesenchymal transition: Implications for diabetic renal disease. *J. Am. Soc. Nephrol.* **2006**, *17*, 2484–2494.
- (19) Lee, C. I.; Guh, J. Y.; Chen, H. C.; Hung, W. C.; Yang, Y. L.; Chuang, L. Y. Advanced glycation end-product-induced mitogenesis and collagen production are dependent on angiotensin II and connective tissue growth factor in NRK-49F cells. *J. Cell Biochem.* **2005**, *95*, 281–292.
- (20) Niu, Y.; Xie, T.; Ge, K.; Lin, Y.; Lu, S. Effects of extracellular matrix glycosylation on proliferation and apoptosis of human dermal fibroblasts via the receptor for advanced glycosylated end products. *Am. J. Dermatopathol.* **2008**, *30*, 344–351.
- (21) Shoji, T.; Koyama, H.; Morioka, T.; Tanaka, S.; Kizu, A.; Motoyama, K.; Mori, K.; Fukumoto, S.; Shioi, A.; Shimogaito, N.; Takeuchi, M.; Yamamoto, Y.; Yonekura, H.; Yamamoto, H.; Nishizawa, Y. Receptor for advanced glycation end products is involved in impaired angiogenic response in diabetes. *Diabetes* **2006**, *55*, 2245–2255.
- (22) Yang, M.; Huang, H.; Li, J.; Huang, W.; Wang, H. Connective tissue growth factor increases matrix metalloproteinase-2 and suppresses tissue inhibitor of matrix metalloproteinase-2 production by cultured renal interstitial fibroblasts. *Wound Repair Regen.* **2007**, *15*, 817–824.
- (23) McLennan, S. V.; Wang, X. Y.; Moreno, V.; Yue, D. K.; Twigg, S. M. Connective tissue growth factor mediates high glucose effects on matrix degradation through tissue inhibitor of matrix metalloproteinase type 1: Implications for diabetic nephropathy. *Endocrinology* **2004**, *145*, 5646–5655.
- (24) Kuge, Y.; Takai, N.; Ishino, S.; Temma, T.; Shiomi, M.; Saji, H. Distribution profiles of membrane type-1 matrix metalloproteinase (MT1-MMP), matrix metalloproteinase-2 (MMP-2) and cyclooxygenase-2 (COX-2) in rabbit atherosclerosis: Comparison with plaque instability analysis. *Biol. Pharm. Bull.* **2007**, *30*, 1634–1640.
- (25) Pawlak, K.; Pawlak, D.; Mysliwiec, M. Serum matrix metalloproteinase-2 and increased oxidative stress are associated with carotid atherosclerosis in hemodialyzed patients. *Atherosclerosis* **2007**, *190*, 199–204.
- (26) Wang, M.; Zhao, D.; Spinetti, G.; Zhang, J.; Jiang, L. Q.; Pintus, G.; Monticone, R.; Lakatta, E. G. Matrix metalloproteinase 2 activation of transforming growth factor- β 1 (TGF- β 1) and TGF- β 1-type II receptor signaling within the aged arterial wall. *Arterioscler., Thromb., Vasc. Biol.* **2006**, *26*, 1503–1509.
- (27) Li, L.; Mamputu, J. C.; Wiernsperher, N.; Renier, G. Signaling pathways involved in human vascular smooth muscle cell proliferation and matrix metalloproteinase-2 expression induced by leptin: Inhibitory effect of metformin. *Diabetes* **2005**, *54*, 2227–2234.
- (28) Huang, J.; Kontos, C. D. Inhibition of vascular smooth muscle cell proliferation, migration, and survival by the tumor suppressor protein PTEN. *Arterioscler., Thromb., Vasc. Biol.* **2002**, *22*, 745–751.
- (29) Dandona, P.; Aljada, A.; Bandyopadhyay, A. Inflammation: The link between insulin resistance, obesity and diabetes. *Trends Immunol.* **2004**, *25*, 4–7.
- (30) Hattori, Y.; Hattori, S.; Sato, N.; Kasai, K. High-glucose-induced nuclear factor κ B activation in vascular smooth muscle cells. *Cardiovasc. Res.* **2000**, *46*, 188–197.
- (31) Lee, S. H.; Woo, H. G.; Baik, E. J.; Moon, C. H. High glucose enhances IL-1 β -induced cyclooxygenase-2 expression in rat vascular smooth muscle cells. *Life Sci.* **2000**, *68*, 57–67.
- (32) Lo, C. W.; Huang, H. P.; Lin, H. M.; Chien, C. T.; Wang, C. J. Effect of *Hibiscus* anthocyanins rich extract induces apoptosis of proliferating smooth muscle cell via activation of p38 MAPK and p53 pathway. *Mol. Nutr. Food Res.* **2007**, *51*, 1452–1460.

Received for review December 17, 2008. Revised manuscript received February 24, 2009. Accepted February 24, 2009. Funding for this research was provided by the National Science Council (NSC), Taiwan, under NSC 97-2320-B-241-003-MY3, and Chung-Shan Medical University Hospital, under CSH-2009-D-001.

JF803911N